Submitted to *Dalton Trans.* June 2019

SUPPORTING INFORMATION

Synthesis, structure and magnetic properties of a series of dinuclear heteroleptic Zn^{2+}/Ln^{3+} Schiff base complexes: effect of the lanthanide ion over the slow relaxation of the magnetization.

Ahlem-Linda Boulkedid,[a,b] Adel Beghidja,[a] Chahrazed Beghidja,[a] Yannick Guari,[b] Joulia Larionova,[b] Jérôme Long*[b]

a. Unité de Recherche de Chimie de l'Environnement et Moléculaire Structurale (CHEMS), Université frères Mentouri Constantine, Route Aïn elbey, 25000 Constantine, (Algérie). E-mail : abeghidja@umc.edu.dz

b. Institut Charles Gerhardt Montpellier, UMR 5253, Ingénierie Moléculaire et Nano-Objets, Université de Montpellier, ENSCM, CNRS, Place E. Bataillon, 34095 Montpellier Cedex 5 (France).

TABLE OF CONTENTS

Experimental Section

General Conditions: All experiments were carried out under aerobic conditions. All the solvents in these experiments were analytical grade. The lanthanide chloride salts were purchased from Alfa Aesar. The ligand H_2L (H_2L = N,N'-bis(3-methoxysalicylidene)-1,2-diaminoethane) has been synthesized according to a well-established procedure from the literature.[1] The purity of H_2L was checked by ^{1}H NMR. Elemental analyses (C, H, N) was carried out with a Perkin-Elmer 2400 elemental analyzer. Infrared spectra were recorded in the range 4000–500 cm^{-1} on a FT-IR Bruker ATR Vertex 70 Spectrometer.

Synthesis of 1-3.

A series of hetero-dinuclear ZnLn complexes **[ZnLClLn(*o*-van)(H_2O)(NO_3)]•H_2O** (Ln = Tb (**1**), Dy (**2**), Er (**3**)) was obtained from the reaction between one equivalent (0.1 mmol) of lanthanide chloride of ($TbCl_3 \cdot 5H_2O$, $DyCl_3 \cdot 5H_2O$, $ErCl_3 \cdot 5H_2O$, weighed respectively: 37.3 mg, 37.6 mg and 38.1 mg) and an equimolar solution of H_2L (0.2 mmol, 65.6 mg) and $Zn(NO_3)_2 \cdot 6H_2O$ (0.2 mmol, 59.4 mg,) in methanol (15 mL). The mixtures were refluxed 5 hours at 60° C. Clear yellow solutions were obtained and were left to evaporate at room temperature. Within 48 h, yellow crystals suitable for single-crystal X-ray diffraction were obtained and separated by filtration. Yield based on Ln^{III}: 42 %, 41 %, 42 % for **1**, **2** and **3** respectively. Elemental Anal. Calcd. $C_{26}H_{29}ClTbN_3O_{12}Zn$ C: 37.38%, H: 3.50%, N: 5.03% Found: C: 37.03, H: 3.62, N: 5.29 for (**1**). Calcd. $C_{26}H_{29}ClDyN_3O_{12}Zn$ C: 37.22%, H: 3.48%, N: 5.01% Found: C: 37.03, H: 3.62, N: 5.29 for (**2**). Calcd. $C_{26}H_{29}ClErN_3O_{12}Zn$ C: 37.01%, H: 3.46%, N: 4.98% Found: C: 37.23, H: 3.62, N: 5.19 for (**3**).

Powder X-Ray diffraction

Powder XRD (PXRD) patterns were measured using a Bruker D8 diffractometer with a copper source operated at 1600 W, with step size = 0.02° and exposure time = 0.5 s per step. PXRD measurements were used to check the purity of the obtained microcrystalline products by a comparison of the experimental results with the calculated patterns obtained from single-crystal XRD data.

Single-crystal X-Ray crystallography

Diffraction intensities for complexes **1**–**3** were collected on a Bruker-AXS APEX II CCD diffractometer at 293(2) K. The crystallographic data, conditions retained for the intensity data collection and some features of the structure refinements are listed in Table S1. The intensities were collected with Mo Kα radiation (λ = 0.71073 Å). Data processing, Lorentz-polarization were performed using APEX.[2] The structure was solved by direct methods and refined by full-matrix least-squares methods on F^2, using the SHELXL-2018 [3] program package. All non-hydrogen atoms were refined anisotropically. Hydrogen atoms in **1**–**3** were placed in calculated positions and were refined in the "riding" model with $U(H)_{iso} = 1.2U_{eq}$ of their parent atoms ($U(H)_{iso} = 1.5U_{eq}$ for methyl groups). Molecular plots were performed with the CrystalMaker and Mercury programs.[4,5] Geometrical calculations were carried out with PLATON.[6] CCDC–1913024 (**1**), 1913022 (**2**) and 1913023 (**3**) contains the supplementary crystallographic data

for this paper. These data are provided free of charge by The Cambridge Crystallographic Data Centre: ccdc.cam.ac.uk/structures.

Magnetic Measurements

Magnetic susceptibility data were collected with a Quantum Design MPMS-XL SQUID magnetometer working in the range 1.8–300 K with the magnetic field up to 7 Tesla. The sample were prepared in a glove box. The data were corrected for the sample holder and the diamagnetic contributions calculated from the Pascal's constants. The AC magnetic susceptibility measurements were carried out in the presence of a 3 Oe oscillating field in zero or applied external DC field.

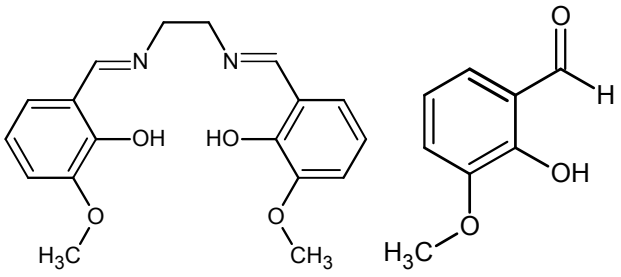

Scheme S1: Chemical structures of H_2L (left) and o-vanH (right).

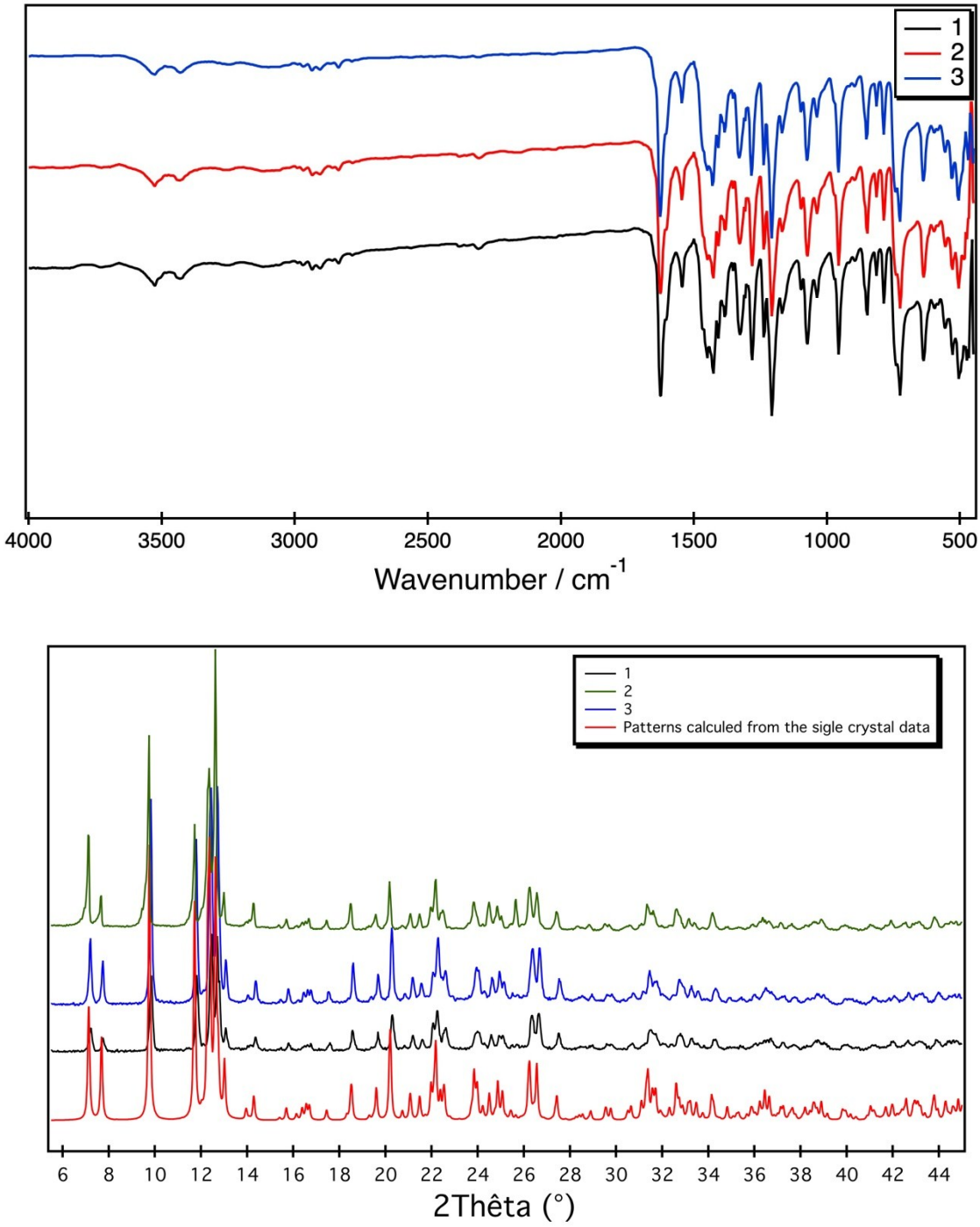

Figure S1: Top: IR spectra for compounds **1-3**. Bottom: Powder X-ray diffraction patterns (Cu Kα1) from experiment and simulated for **1-3**.

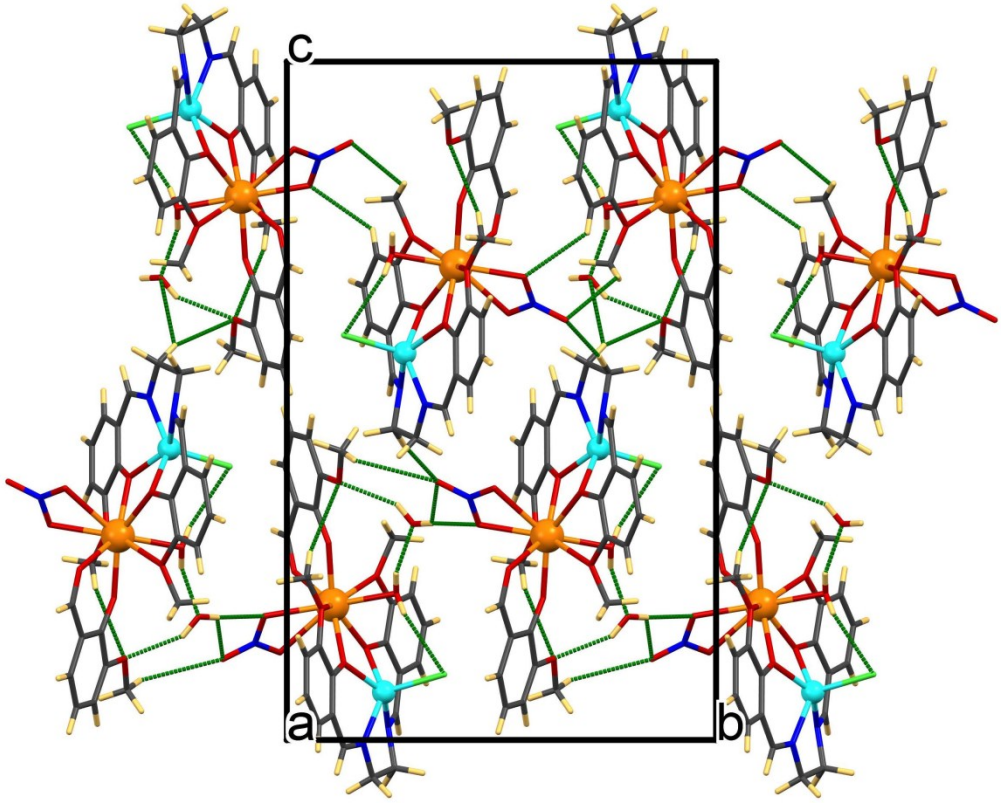

Figure S2: Perspective view of the crystal packing for **2** along the *a* crystallographic axis. The hydrogen bonding is indicated by green dashed lines.

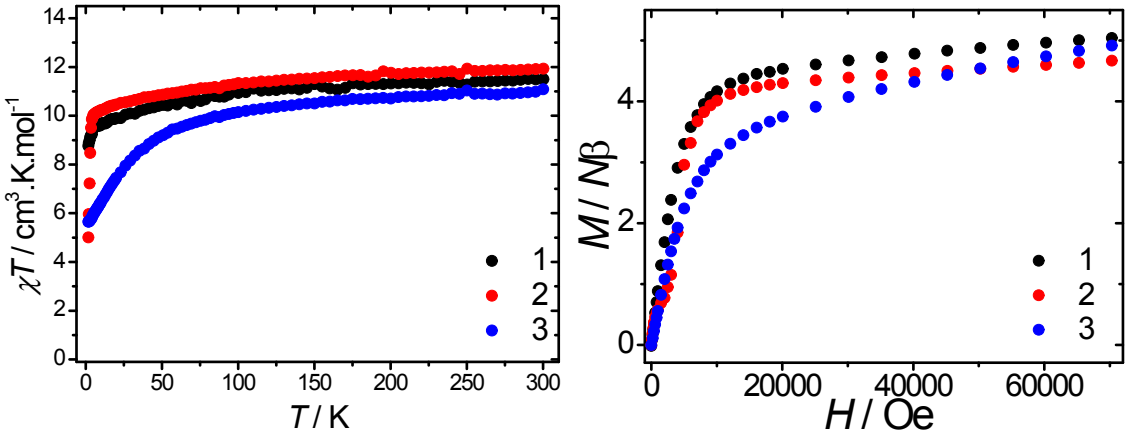

Figure S3: Left: temperature dependence of χT under an applied magnetic field of 1000 Oe for **1-3**. Right: field dependence of the magnetization at 1.8 K for **1-3**.

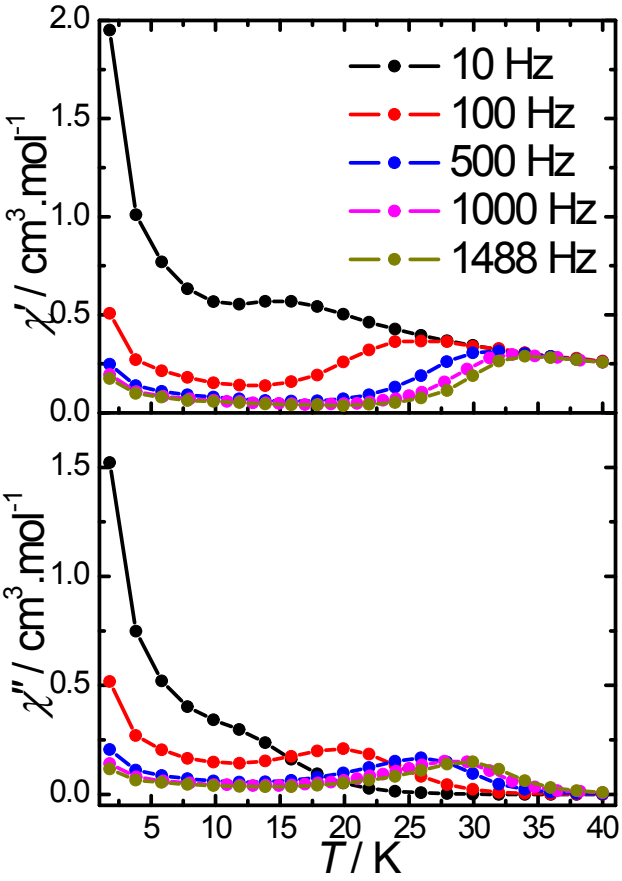

Figure S4. Temperature dependence of χ' and χ'' for **2** for different frequencies.

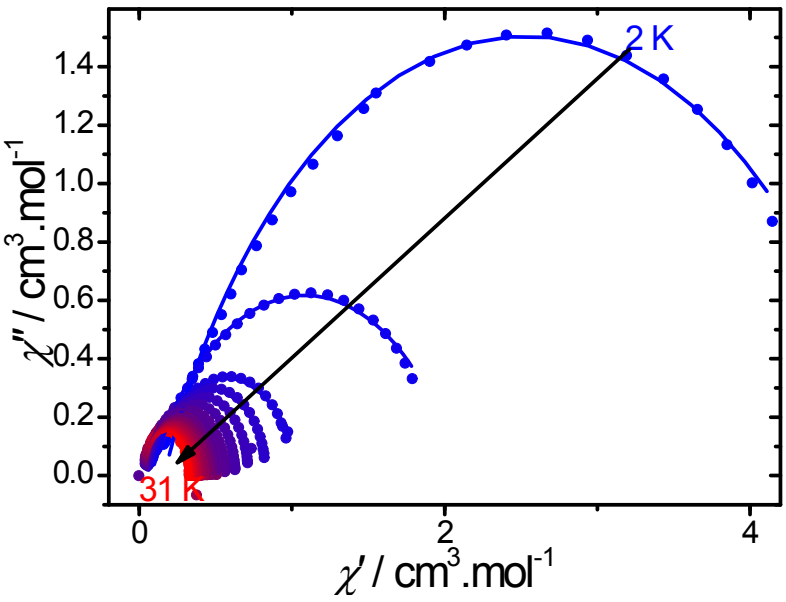

Figure S5: Cole-Cole (Argand) plots obtained using the ac susceptibility data for **2** (0 Oe). The solid lines correspond to the best fit obtained with a generalized Debye model.

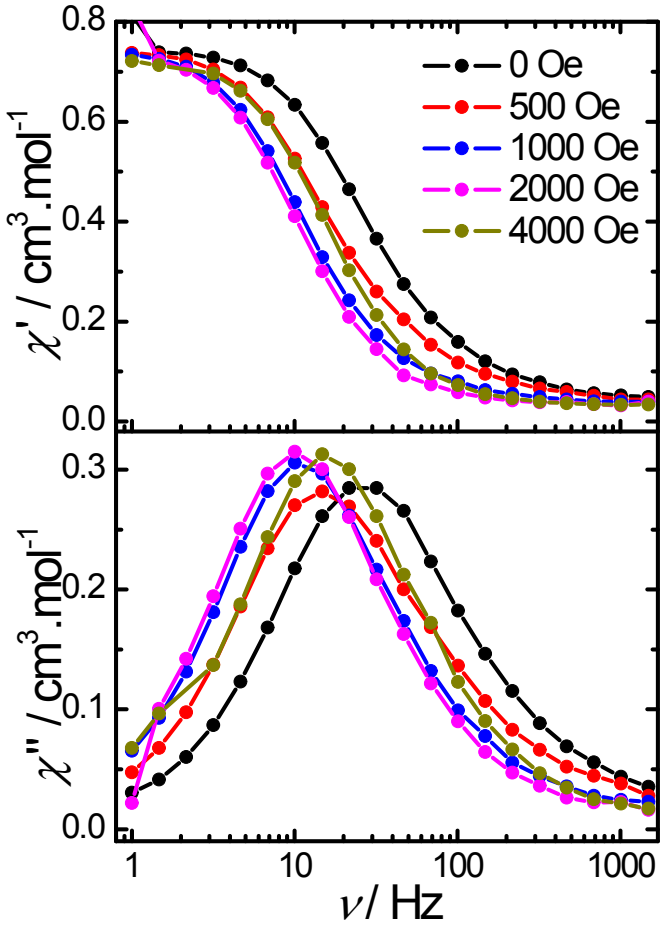

Figure S6. Frequency dependence of χ' and χ'' for **2** at 15 K for various dc fields.

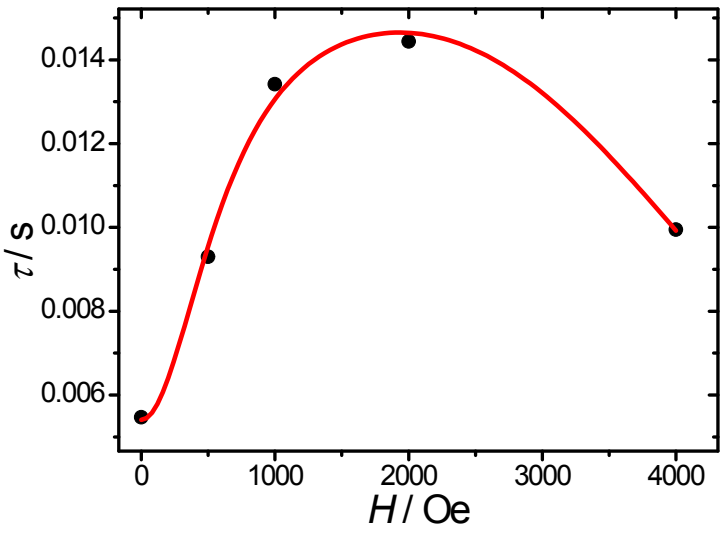

Figure S7. Field dependence of the relaxation time for **2** at 15 K. The solid line represents the fit with Eq. 2.

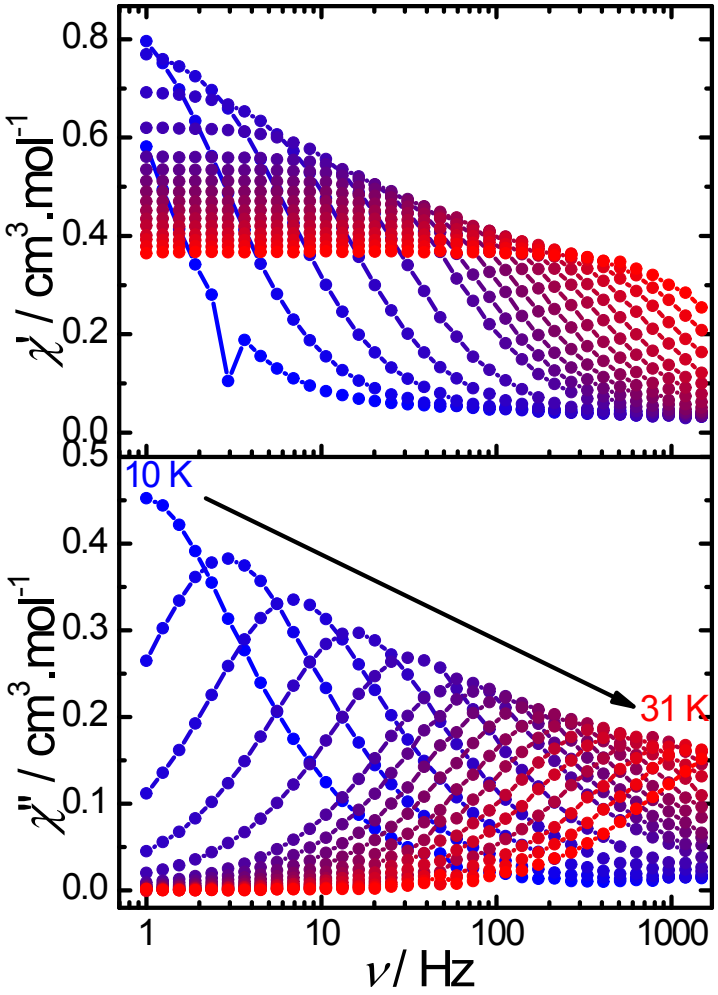

Figure S8. Frequency dependence of χ' and χ'' for **2** under a 2000 Oe dc field.

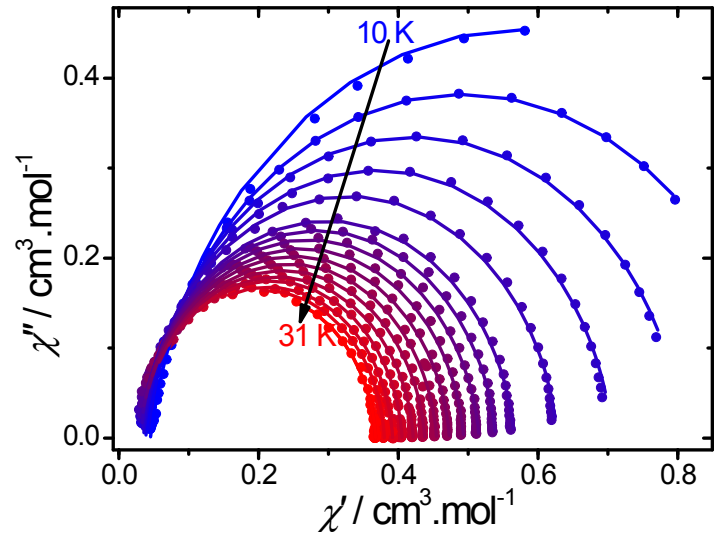

Figure S9: Cole-Cole (Argand) plots obtained using the ac susceptibility data for **2** (2000 Oe) The solid lines correspond to the best fit obtained with a generalized Debye model.

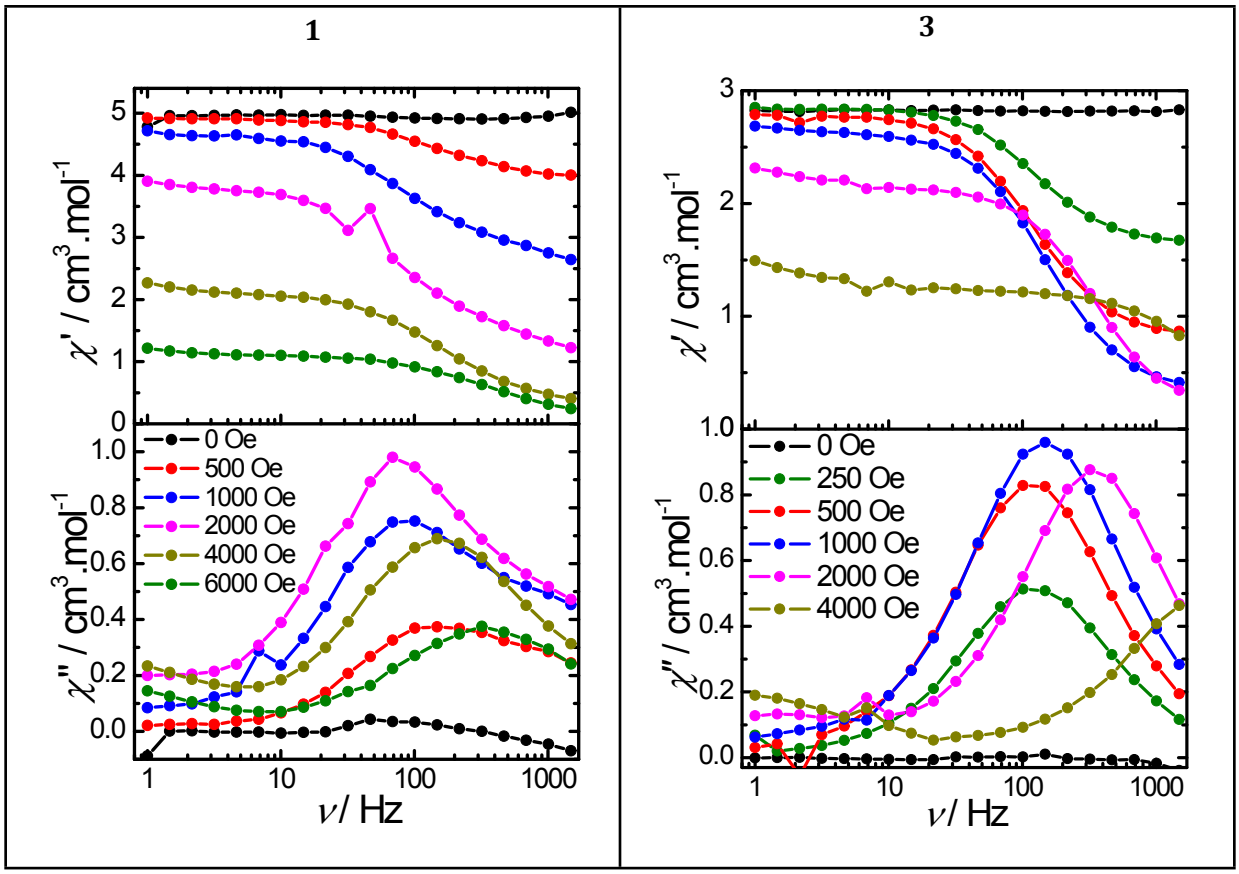

Figure S10. Frequency dependence of χ' and χ'' at 2 K under various dc fields for **1** and **3**.

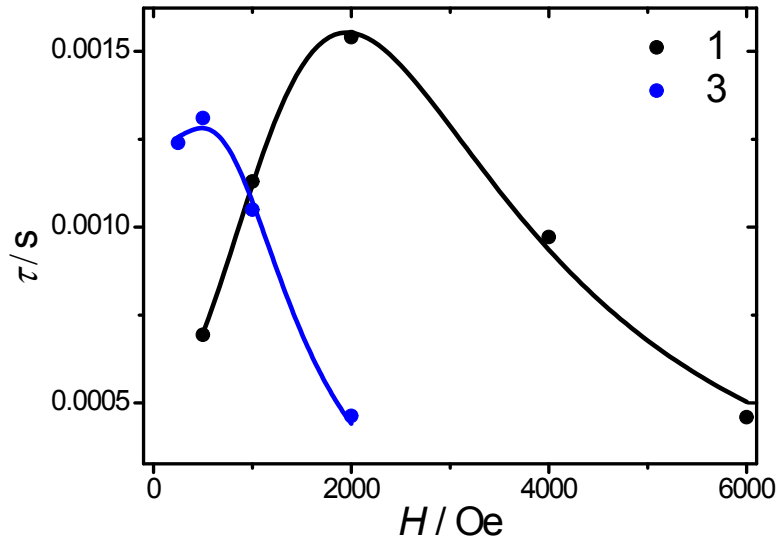

Figure S11. Field dependence of the relaxation time for **1** and **3** at 2 K. The solid lines represent the fit with Eq. 2.

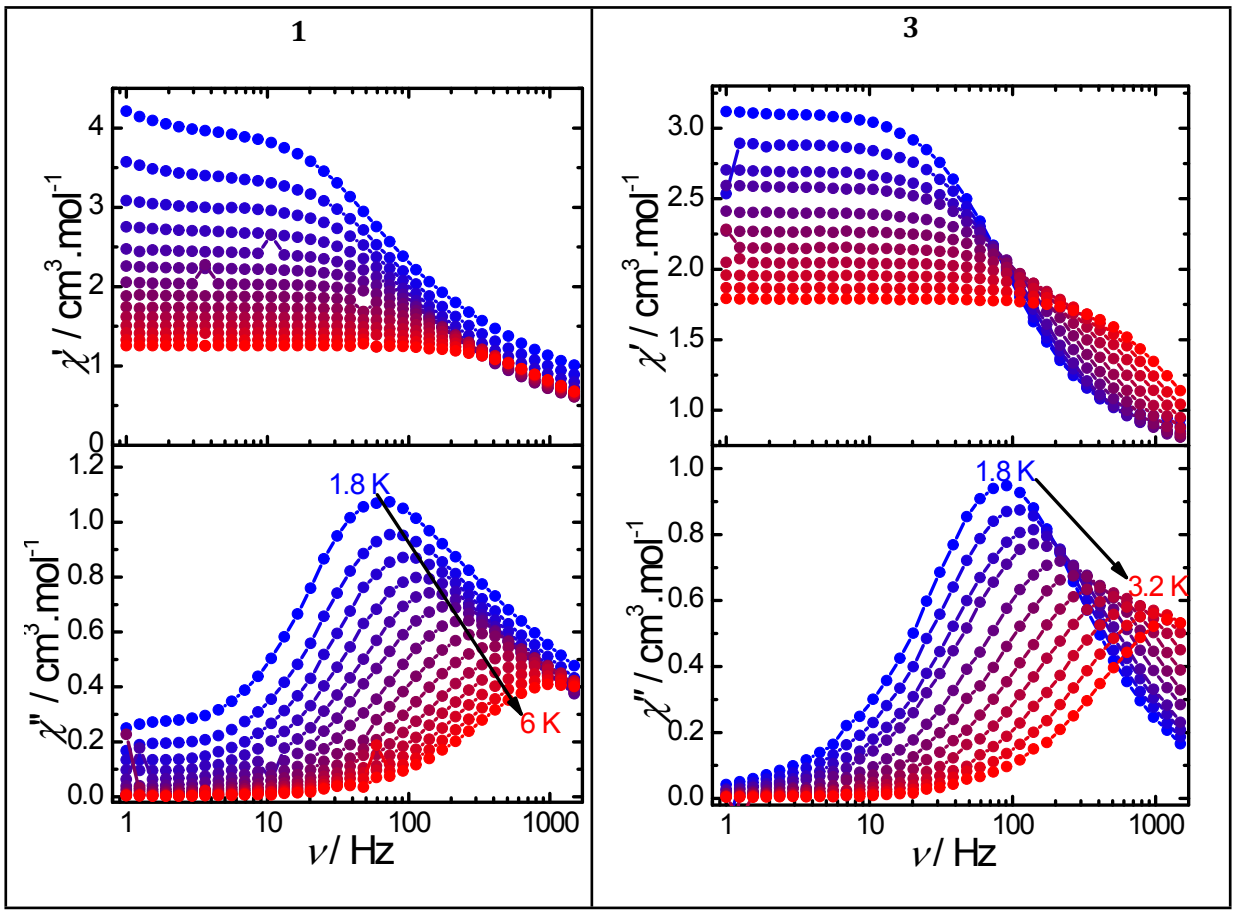

Figure S12. Frequency dependence of χ' and χ'' for **1** (2000 Oe) and **3** (500 Oe).

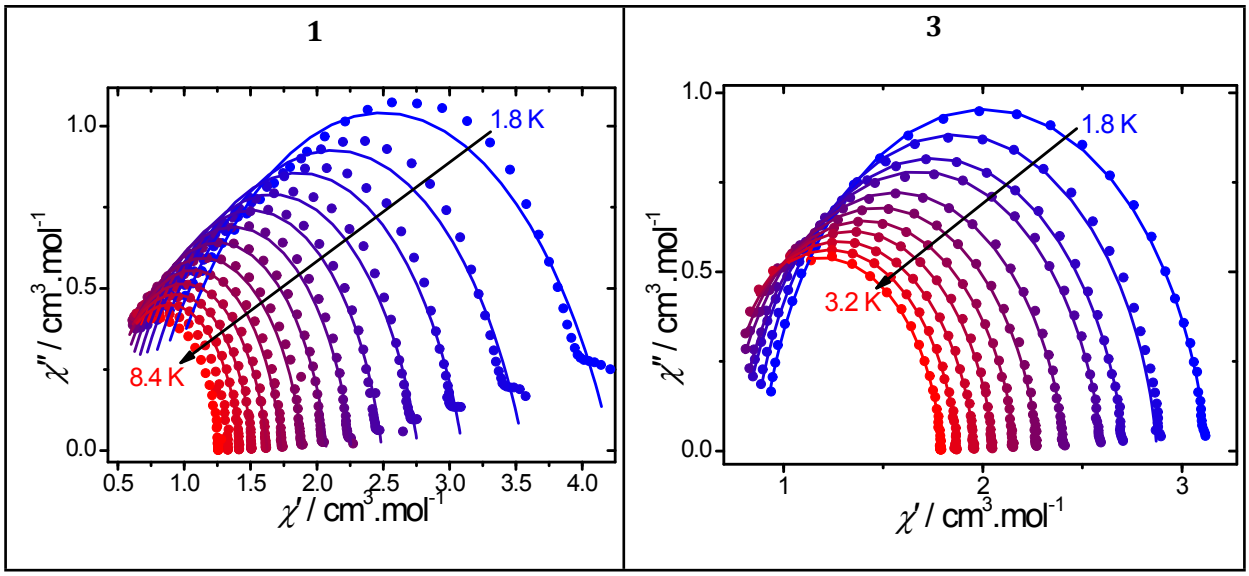

Figure S13. Cole-Cole (Argand) plots obtained using the ac susceptibility data for **1** (2000 Oe) and **3** (500 Oe). The solid lines correspond to the best fit obtained with a generalized Debye model.

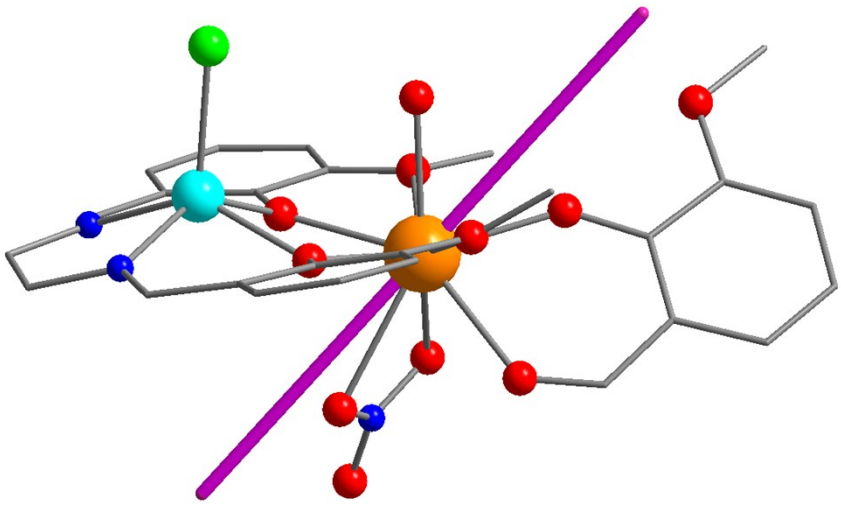

Figure S14. Orientation of the anisotropic axis (purple) for **2** obtained with the MAGELLAN software.[2]

Table S1. The crystal data and structures refinement details for complexes **1**–**3.**

Identification code	**1**	**2**	**3**
Empirical formula	$C_{26}H_{29}ClN_3O_{12}TbZn$	$C_{26}H_{29}ClDyN_3O_{12}Zn$	$C_{26}H_{29}ClErN_3O_{12}Zn$
Formula weight	834.25	838.84	843.60
Temperature/K	296.15	296.15	273.15
Crystal system	monoclinic	monoclinic	monoclinic
Space group	$P2_1/c$	$P2_1/c$	$P2_1/c$
a/Å	8.7869(2)	8.764(2)	8.7916(5)
b/Å	14.7296(3)	14.599(5)	14.7051(7)
c/Å	23.0656(4)	23.079(8)	22.9881(13)
α/°	90	90	90
β/°	90.5950(10)	91.124(15)	90.723(2)
γ/°	90	90	90
Volume/Å^3	2985.16(10)	2952.3(16)	2971.7(3)
Z	4	4	4
ρ_{calc}g/cm^3	1.856	1.887	1.886
μ/mm^{-1}	3.310	3.483	3.769
F(000)	1652.0	1660.0	1668.0
Crystal size/mm^3	0.18 × 0.15 × 0.11	0.18 × 0.16 × 0.13	0.16 × 0.14 × 0.1
Radiation	MoKα (λ = 0.71073)	MoKα (λ = 0.71073)	MoKα (λ = 0.71073)
2Θ range for data collection/°	7.59 to 66.282	7.456 to 56.562	6.428 to 61.192
Index ranges	$-12 \le h \le 13$, $-22 \le k \le 22$, $-35 \le l \le 35$	$-11 \le h \le 11$, $-19 \le k \le 8$, $-30 \le l \le 30$	$-12 \le h \le 12$, $-21 \le k \le 20$, $-31 \le l \le 32$
Reflections collected	80993	18007	34543
Independent reflections	11365 [R_{int} = 0.0267, R_{sigma} = 0.0177]	7034 [R_{int} = 0.0292, R_{sigma} = 0.0383]	9047 [R_{int} = 0.0984, R_{sigma} = 0.1054]
Data/restraints/parameters	11365/6/413	7034/0/402	9047/0/413
Goodness-of-fit on F^2	1.094	1.020	1.030
Final R indexes [I>=2σ (I)]	R_1 = 0.0299, wR_2 = 0.0720	R_1 = 0.0297, wR_2 = 0.0769	R_1 = 0.0583, wR_2 = 0.1530
Final R indexes [all data]	R_1 = 0.0396, wR_2 = 0.0768	R_1 = 0.0414, wR_2 = 0.0830	R_1 = 0.0777, wR_2 = 0.1663
Largest diff. peak/hole / e Å^{-3}	1.09/-0.82	1.06/-1.12	1.77/-1.71

Table S2. Bond distances (in Å) for the two crystallographically independent metallic coordination environments present in compounds **1-3**

1		**2**		**3**	
Atom—Atom	**Length (Å)**	**Atom—Atom**	**Length (Å)**	**Atom—Atom**	**Length (Å)**
Tb1—O1W	2.368 (2)	Dy1—O1W	2.344 (3)	Er1—O1W	2.327 (4)
Tb1—O1	2.6765 (19)	Dy1—O1	2.692 (3)	Er1—O1	2.686 (4)
Tb1—O2	2.2979 (17)	Dy1—O2	2.311 (3)	Er1—O2	2.270 (4)
Tb1—O3	2.3126 (17)	Dy1—O3	2.272 (2)	Er1—O3	2.264 (3)
Tb1—O4	2.7000 (17)	Dy1—O4	2.672 (3)	Er1—O4	2.692 (4)
Tb1—O5	2.2211 (17)	Dy1—O5	2.416 (3)	Er1—O5	2.181 (4)
Tb1—O6	2.4255 (19)	Dy1—O6	2.201 (3)	Er1—O6	2.385 (4)
Tb1—O8	2.609 (2)	Dy1—O8	2.457 (3)	Er1—O8	2.586 (5)
Tb1—O9	2.4876 (19)	Dy1—O9	2.588 (3)	Er1—O9	2.435 (4)
Zn1—Cl1	2.2792 (8)	Zn1—Cl1	2.2633 (14)	Zn1—Cl1	2.2793 (16)
Zn1—O2	2.0494 (16)	Zn1—O2	2.019 (3)	Zn1—O2	2.037 (4)
Zn1—O3	2.0345 (18)	Zn1—O3	2.051 (2)	Zn1—O3	2.046 (4)
Zn1—N1	2.042 (3)	Zn1—N1	2.045 (3)	Zn1—N1	2.031 (5)
Zn1—N2	2.044 (2)	Zn1—N2	2.031 (4)	Zn1—N2	2.050 (5)

Table S3. Bond angles (in degrees) for the two crystallographically independent metallic coordination environments present in compounds **1-3**

1			
Atom—Atom—Atom	**Angles (º)**	**Atom—Atom—Atom**	**Angles (º)**
O1W—Tb1—O2	80.69 (7)	O3—Tb1—O6	145.97 (6)
O1W—Tb1—O3	80.09 (7)	O3—Tb1—O8	75.33 (6)
O1W—Tb1—O4	78.66 (8)	O3—Tb1—O9	83.68 (7)
O1W—Tb1—O5	78.32 (7)	O4—Tb1—O5	76.06 (6)
O1W—Tb1—O6	131.20 (7)	O4—Tb1—O6	129.29 (6)
O1W—Tb1—O8	150.47 (7)	O4—Tb1—O8	102.81 (6)
O1W—Tb1—O9	143.11 (7)	O4—Tb1—O9	64.51 (6)
O1W—Tb1—O1	70.81 (7)	O5—Tb1—O6	73.28 (7)
O1—Tb1—O2	61.64 (6)	O5—Tb1—O8	131.00 (7)
O1—Tb1—O3	124.62 (6)	O5—Tb1—O9	90.42 (7)
O1—Tb1—O4	146.39 (6)	O6—Tb1—O8	70.72 (6)
O1—Tb1—O5	84.17 (6)	O6—Tb1—O9	76.29 (6)
O1—Tb1—O6	67.57 (6)	O8—Tb1—O9	49.56 (6)
O1—Tb1—O8	110.66 (6)	Cl1—Zn1—O2	106.13 (5)
O1—Tb1—O9	143.50 (6)	Cl1—Zn1—O3	108.16 (6)
O2—Tb1—O3	67.99 (6)	Cl1—Zn1—N1	110.52 (9)
O2—Tb1—O4	127.24 (6)	Cl1—Zn1—N2	114.67 (7)
O2—Tb1—O5	144.27 (7)	O2—Zn1—O3	78.28 (7)
O2—Tb1—O6	100.44 (6)	O2—Zn1—N1	85.98 (8)
O2—Tb1—O8	75.12 (6)	O2—Zn1—N2	139.16 (8)

O2—Tb1—O9	122.92 (7)	O3—Zn1—N1	140.93 (10)
O3—Tb1—O4	60.92 (6)	O3—Zn1—N2	87.10 (8)
O3—Tb1—O5	134.76 (6)	N1—Zn1—N2	81.85 (10)

2			
Atom—Atom—Atom	**Angles (º)**	**Atom—Atom—Atom**	**Angles (º)**
O1W—Dy1—O1	78.57 (9)	O3—Dy1—O6	144.08 (9)
O1W—Dy1—O2	80.12 (10)	O3—Dy1—O8	122.84 (9)
O1W—Dy1—O3	80.51 (9)	O3—Dy1—O9	74.81 (9)
O1W—Dy1—O4	70.82 (9)	O4—Dy1—O5	67.06 (9)
O1W—Dy1—O5	131.23 (10)	O4—Dy1—O6	83.35 (9)
O1W—Dy1—O6	78.69 (10)	O4—Dy1—O8	143.57 (9)
O1W—Dy1—O8	143.00 (9)	O4—Dy1—O9	110.77 (8)
O1W—Dy1—O9	150.01 (10)	O5—Dy1—O6	73.19 (9)
O1—Dy1—O2	60.62 (9)	O5—Dy1—O8	76.78 (9)
O1—Dy1—O3	127.05 (8)	O5—Dy1—O9	70.75 (9)
O1—Dy1—O4	146.09 (8)	O6—Dy1—O8	90.62 (10)
O1—Dy1—O5	129.85 (9)	O6—Dy1—O9	131.14 (10)
O1—Dy1—O6	76.55 (9)	O8—Dy1—O9	49.85 (9)
O1—Dy1—O8	64.46 (8)	Cl1—Zn1—O2	107.86 (8)
O1—Dy1—O9	103.01 (8)	Cl1—Zn1—O3	105.52 (7)
O2—Dy1—O3	68.18 (8)	Cl1—Zn1—N1	114.50 (9)
O2—Dy1—O4	125.35 (9)	Cl1—Zn1—N2	110.32 (9)
O2—Dy1—O5	145.77 (9)	O2—Zn1—O3	78.25 (9)
O2—Dy1—O6	135.07 (9)	O2—Zn1—N1	87.84 (11)
O2—Dy1—O8	83.19 (9)	O2—Zn1—N2	141.44 (11)
O2—Dy1—O9	75.10 (9)	O3—Zn1—N1	139.95 (11)
O3—Dy1—O4	62.20 (8)	O3—Zn1—N2	86.59 (11)
O3—Dy1—O5	100.08 (8)	N1—Zn1—N2	81.34 (14)

3			
Atom—Atom—Atom	**Angles (º)**	**Atom—Atom—Atom**	**Angles (º)**
O1W—Er1—O1	78.11 (14)	O3—Er1—O6	98.35 (13)
O1W—Er1—O2	80.24 (16)	O3—Er1—O8	74.48 (13)
O1W—Er1—O3	81.38 (14)	O3—Er1—O9	122.98 (14)
O1W—Er1—O4	70.76 (14)	O4—Er1—O5	82.48 (15)
O1W—Er1—O5	78.27 (16)	O4—Er1—O6	67.00 (14)
O1W—Er1—O6	131.76 (15)	O4—Er1—O8	111.72 (13)
O1W—Er1—O8	149.88 (15)	O4—Er1—O9	143.73 (14)
O1W—Er1—O9	142.51 (15)	O5—Er1—O6	74.19 (15)
O1—Er1—O2	61.51 (13)	O5—Er1—O8	131.61 (15)
O1—Er1—O3	128.67 (13)	O5—Er1—O9	90.65 (16)
O1—Er1—O4	145.01 (13)	O6—Er1—O8	70.50 (14)
O1—Er1—O5	75.80 (15)	O6—Er1—O9	76.84 (15)
O1—Er1—O6	129.97 (13)	O8—Er1—O9	50.00 (14)
O1—Er1—O8	103.21 (13)	Cl1—Zn1—O2	108.33 (13)

O1—Er1—O9	64.43 (14)	Cl1—Zn1—O3	106.38 (10)
O2—Er1—O3	68.93 (13)	Cl1—Zn1—N1	114.53 (14)
O2—Er1—O4	125.78 (14)	Cl1—Zn1—N2	111.15 (17)
O2—Er1—O5	135.20 (15)	O2—Zn1—O3	77.87 (14)
O2—Er1—O6	144.86 (14)	O2—Zn1—N1	86.91 (17)
O2—Er1—O8	74.50 (14)	O2—Zn1—N2	140.1 (2)
O2—Er1—O9	83.18 (15)	O3—Zn1—N1	139.02 (16)
O3—Er1—O4	62.28 (13)	O3—Zn1—N2	85.90 (17)
O3—Er1—O5	143.56 (15)	N1—Zn1—N2	81.9 (2)

Table S4. Hydrogen bonding geometrical details (distances in Å and angles in degrees) for compounds **1-3**

1				
D*—H···*A	***D*—H**	**H···*A***	***D*···*A***	***D*—H···*A***
O1*W*—H1*WA*···Cl1	0.87	2.38	3.219 (2)	165
O1*W*—H1*WB*···O2*W*	0.90	1.85	2.647 (4)	147
O2*W*—H2*WA*···O9^{i}	0.85	2.17	2.993 (3)	163
O2*W*—H2*WA*···O10^{i}	0.85	2.50	3.173 (4)	137
O2*W*—H2*WB*···O7	0.85	2.53	2.936 (4)	110
C18—H18*C*···O5	0.96	2.51	3.188 (3)	127
C9*B*—H9*BA*···O10^{ii}	0.97	2.57	3.533 (8)	174
Symmetry codes : (i) -*x*+1, *y*+1/2, -*z*+1/2; (ii) -*x*, -*y*, -*z*.				

2				
D*—H···*A	***D*—H**	**H···*A***	***D*···*A***	***D*—H···*A***
O1*W*—H1*WA*···Cl1	0.86	2.58	3.202 (3)	131
O1*W*—H1*WB*···O2*W*	0.86	1.86	2.639 (5)	151
O2*W*—H2*WA*···O8^{i}	0.85	2.13	2.979 (5)	176
O2*W*—H2*WA*···O10^{i}	0.85	2.53	3.140 (5)	129
O2*W*—H2*WB*···O7	0.85	2.15	2.918 (5)	151
C1—H1*A*···O6	0.96	2.50	3.180 (5)	128
Symmetry codes : (i) -*x*, *y*+1/2, -*z*+1/2.				

3				
D*—H···*A	***D*—H**	**H···*A***	***D*···*A***	***D*—H···*A***
O1*W*—H1*WA*···Cl1	0.88	2.50	3.207 (5)	138
O1*W*—H1*WB*···O2*W*	0.88	1.78	2.645 (8)	171
O2*W*—H2*WA*···O7	0.85	2.10	2.927 (8)	165
O2*W*—H2*WB*···O9^{i}	0.85	2.35	3.028 (8)	138
O2*W*—H2*WB*···O10^{i}	0.85	2.35	3.168 (9)	162
C1—H1*C*···O5	0.96	2.50	3.166 (8)	127
C10*A*—H10*B*···O10^{ii}	0.97	2.56	3.528 (18)	176
Symmetry codes : (i) -*x*, *y*+1/2, -*z*+1/2; (ii) -*x*+1, -*y*, -*z*+1.				

Table S5. SHAPE analysis for compounds **1-3**
(The deviation of the atom arrangement of coordination polyhedron from an ideal spherical capped square antiprism).

	Complex 1	Complex 2	Complex 3
	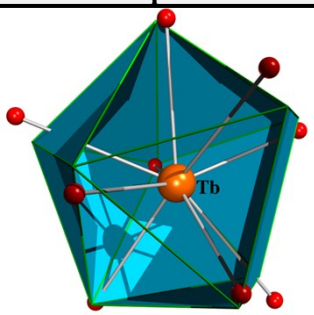	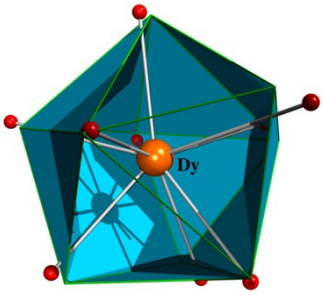	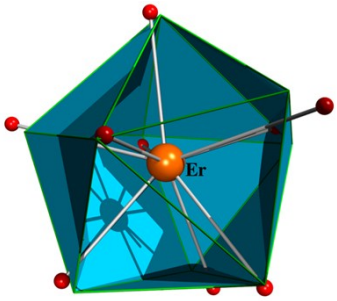
JCCU	7.666	7.655	7.753
CCU	6.908	6.929	7.106
JCSAPR	2.874	2.847	2.780
CSAPR	**2.466**	**2.467**	**2.457**
JTCTPR	3.452	3.363	3.049
TCTPR	3.400	3.399	3.316

JCCU: Capped cube
CCU: Spherical-relaxed capped cube
JCSAPR: Capped square antiprism
CSAPR: Spherical capped square antiprism
JTCTPR: Tricapped trigonal prism
TCTPR: Spherical tricapped trigonal prism

Table S6. Fitting of the Cole-Cole plots with a generalized Debye model under a zero dc field for **2**.

T (K)	χ_S (cm^3. mol^{-1})	χ_T (cm^3. mol^{-1})	α
2	0.16117	4.89953	0.27954
5	0.07726	2.09058	0.29934
10	0.05636	1.06483	0.25361
12	0.05518	0.86326	0.19357

14	0.04714	0.74113	0.1609
16	0.04227	0.64053	0.1231
18	0.04509	0.52292	0.03041
20	0.03281	0.51132	0.08356
21	0.03279	0.48728	0.07377
22	0.0325	0.46769	0.06974
23	0.03075	0.44499	0.06745
24	0.03432	0.42433	0.04364
25	0.03321	0.40599	0.0388
26	0.02981	0.39403	0.04652
27	0.02916	0.38017	0.04376
28	0.02718	0.36668	0.04002
29	0.02616	0.35418	0.03663
30	0.02041	0.34285	0.036
31	4.70461E-15	0.3367	0.06878

Table S7: Some examples of high energy barriers Zn/Dy SMMS**.**

Nuclearity	U_{eff} (cm^{-1}), H = 0 Oe	Reference
ZnDy	233	[3]
ZnDy	83	[4]
Zn_2Dy	89	[5]
Zn_2Dy	149	[5]
Zn_2Dy	140	[5]
Zn_2Dy	186	[6]
ZnDy	189	[7]
Zn_2Dy	298	[8]
Zn_2Dy	161	[8]
Zn2Dy	86	[9]

Table S8: Fit parameters of the field dependence of the relaxation time at 6 K for **1-3.**

Compound	*D* ($s^{-1}K^{-1}Oe^{-4}$)	B_1 (s^{-1})	B_2 (Oe^{-2})	*K*
1 (2 K)	2.4×10^{-5}	1722.9	1.9×10^{-6}	255
2 (15 K)	9.8×10^{-15}	123.03	7.5×10^{-6}	61.95
3 (2 K)	1.3×10^{-5}	810.4	9.9×10^{-7}	-

Table S9. Fitting of the Cole-Cole plots with a generalized Debye model under a 2000 Oe field for **2**.

T (K)	χ_S (cm^3. mol^{-1})	χ_T (cm^3. mol^{-1})	α
10	0.04528	1.10504	0.15844
12	0.03825	0.94637	0.05494
14	0.03505	0.80927	0.02239
16	0.03328	0.70652	0.01
18	0.03117	0.62743	0.00478
20	0.03	0.56601	0.00243
21	0.02942	0.5395	0.00177
22	0.02974	0.51561	0.0013
23	0.03062	0.49366	9.69631E-4
24	0.0302	0.47313	7.18017E-4
25	0.03227	0.4548	5.38383E-4
26	0.03218	0.43778	3.97852E-4
27	0.03352	0.42139	2.95942E-4
28	0.03178	0.40531	2.12712E-4
29	0.03606	0.39177	1.54137E-4
30	0.03399	0.37987	1.09211E-4
31	0.02068	0.36753	7.15328E-5

Table S10. Fitting of the Cole-Cole plots with a generalized Debye model under a 2000 Oe field for **1**.

T (K)	**χ_S (cm^3. mol^{-1})**	**χ_T (cm^3. mol^{-1})**	**α**
1.8	0.89223	3.12505	0.09939
1.94	0.84643	2.87469	0.08757
2.08	0.78732	2.71067	0.10264
2.23	0.76177	2.59838	0.10283
2.36	0.71361	2.41243	0.10245
2.5	0.67881	2.27719	0.10234
2.64	0.64969	2.16491	0.10368
2.77	0.63121	2.05357	0.09293
2.92	0.60975	1.95839	0.08901
3.06	0.59866	1.86923	0.0774
3.2	0.59147	1.79133	0.06621

Table S11. Fitting of the Cole-Cole plots with a generalized Debye model under a 500 Oe field for **3**.

T (K)	**χ_S (cm^3. mol^{-1})**	**χ_T (cm^3. mol^{-1})**	**α**
1.8	0.75528	4.22564	0.31175
2.3	0.68203	3.56107	0.2724

2.81	0.62991	3.10083	0.22851
3.31	0.56641	2.76432	0.20665
3.83	0.52918	2.49092	0.17629
4.33	0.48273	2.26124	0.16031
4.85	0.43826	2.07209	0.15242
5.35	0.39289	1.89337	0.14723
5.87	0.40552	1.72943	0.11003
6.36	0.36526	1.62464	0.12699
6.88	0.35416	1.51406	0.11706
7.38	0.35215	1.4199	0.10752

References

1 X. Lu, W. Bi, W. Chai, J. Song, J. Meng, W.-Y. Wong, W.-K. Wong and R. A. Jones, *New. J. Chem.*, 2008, **32**, 127-131.

2 N. F. Chilton, D. Collison, E. J. L. McInnes, R. E. P. Winpenny and A. Soncini, *Nat. Commun.*, 2013, **4**, 2551.

3 A. Watanabe, A. Yamashita, M. Nakano, T. Yamamura and T. Kajiwara, *Chem. Eur. J.*, 2011, **17**, 7428-7432.

4 A. Upadhyay, S. K. Singh, C. Das, R. Mondol, S. K. Langley, K. S. Murray, G. Rajaraman and M. Shanmugam, *Chem. Commun.*, 2014, **50**, 8838-8841.

5 J. P. Costes, S. Titos-Padilla, I. Oyarzabal, T. Gupta, C. Duhayon, G. Rajaraman and E. Colacio, *Chem. Eur. J.*, 2015, **21**, 15785-15796.

6 I. Oyarzabal, J. Ruiz, E. Ruiz, D. Aravena, J. M. Seco and E. Colacio, *Chem. Commun.*, 2015, **51**, 12353-12356.

7 A. Amjad, A. M. Madalan, M. Andruh, A. Caneschi and L. Sorace, *Chem. Eur. J.*, 2016, **22**, 12849-12858.

8 W.-B. Sun, P.-F. Yan, S.-D. Jiang, B.-W. Wang, Y.-Q. Zhang, H.-F. Li, P. Chen, Z.-M. Wang and S. Gao, *Chem. Sci.*, 2016, **7**, 684-691.

9 H.-R. Wen, P.-P. Dong, S.-J. Liu, J.-S. Liao, F.-Y. Liang and C.-M. Liu, *Dalton Trans.*, 2017, **46**, 1153-1162.